

Buckling behavior of functionally graded porous plates integrated with laminated composite faces sheets

Kuo Xu^a, Yuan Yuan^{*a} and Mingyang Li^b

School of Mechanical and Precision Instrument Engineering, Xi'an University of Technology, Xi'an, 710048, China

(Received April 15, 2019, Revised June 10, 2019, Accepted July 9, 2019)

Abstract. In this work, lightweight sandwich plates consisting of a functionally graded porous (FGP) core and two laminated composite face sheets resting on elastic foundation have been proposed. Three different profiles are considered for the distributions of porosities along core thickness. The main aim of this paper is the investigation of the buckling behavior of the proposed porous sandwich plates (PSPs) by reporting their critical mechanical loads and their corresponding mode shapes. A finite element method (FEM) based on first order shear deformation theories (FSDT) is developed to discretize governing equations for the buckling behavior of the proposed sandwich plates. The effects of porosity dispersion and volume, the numbers and angles of laminated layers, sandwich plate geometrical dimensions, elastic foundation coefficients, loading and boundary conditions are studied. The results show that the use of FGP core can offer a PSP with half weight core and only 5% reduction in critical buckling loads. Moreover, stacking sequences with only $\pm 45^\circ$ orientation fibers offer the highest values of buckling loads.

Keywords: sandwich plates; functionally graded porous core; laminated composites; buckling behaviors; FEM

1. Introduction

Insertion of one thicker and softer core between the stacking sequence of laminated composites provides sandwich structures with usually better stiffness, energy absorption, thermal behavior and vibration damping in comparison with regular laminated composites (Birmana and Kardomateas 2018). All these advantages offer sandwich structures with extreme applications in civil, military and aerospace fields. Furthermore, such sandwich structures usually have high strength-to-weight ratio which is their main advantage. Therefore, in order to increase strength-to-weight ratio, the reduction of structural weight could be an important goal in the design of such sandwich structures. In this regard, employing lightweight porous or FGP core instead of perfect core could be an applicable solution because the main contributions of core layer in the mentioned sandwich structures are resisting shear loads and establishing sufficient distance between outer layers (Aram and Mehdipour-Ataei 2016, Shahsavari *et al.* 2018, Shokri-Oojghaz *et al.* 2019). The concept of FG distribution of fillers or porosities was came from functionally graded materials (FGMs) (Tornabene *et al.* 2009, 2011, 2015, Tornabene and Reddy 2013). The use of this concept in the distributions of fillers or porosities was resulted in a significant improvement in the mechanical behavior the resulted FG engineering structures (Frikha *et al.* 2018, Moradi-Dastjerdi and Pourasghar 2016, Pourasghar *et al.* 2018, Pourasghar and Chen 2016, 2019a, b, c).

Buckling analysis of engineering structures has been frequently considered by researchers. The free vibration and buckling behaviors of beams (Malekzadeh and Karami 2008) and plates (Dehghan and Baradaran 2011) resting on elastic foundations have been investigated using an FEM in combination with differential quadrature (DQ) method. Zhao *et al.* (2009) presented thermal buckling analysis for plates made of functionally graded materials using an FSDT based element-free method. Topal (2012) developed a nine-node FEM based on FSDT to optimize the critical buckling temperature of laminated composite plates. Thermal and mechanical buckling analyses of laminated composite plates have been presented using meshless method based on higher order shear deformation theory (HSDT) of plates (Singh *et al.* 2013). The buckling behavior of circular plates made of laminated composites resting on one-parameter elastic foundations has been studied using Ritz method in (Afsharmanesh *et al.* 2014). Zhang *et al.* (2015) presented buckling analysis of skew nanocomposite plates reinforced with FG distribution of carbon nanotubes (CNTs) using FSDT and meshless method. The effect of CNT parameters on the dynamic stability of nanocomposite columns using DQ method was reported in (Pourasghar and Kamarian 2015). The buckling analysis of laminated composite plates including some holes has been conducted using an isogeometric FEM and refined shear deformation theory (RSDT) by (Yu *et al.* 2016). Fattahi and Safaei (2017) considered CNT-reinforced nanocomposite beams with arbitrary boundary conditions and investigated their buckling behaviors using various beam's theories. Moradi-Dastjerdi and Malek-Mohammadi (2017a) studied the free vibration and buckling behavior of FG nanocomposite plates reinforced with CNT agglomerations using an RSDT based analytical method. The effect of CNT agglomerations

*Corresponding author, Associate Professor,
E-mail: yuan yuan.xi.edu@gmail.com

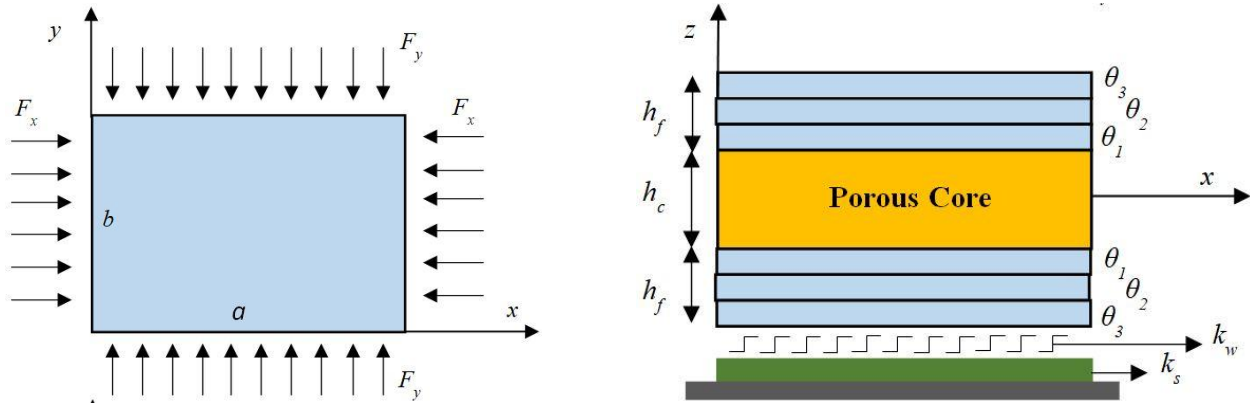


Fig. 1 The schematic of $[\theta_1, \theta_2, \theta_3]$ sandwich plates with a porous core and two laminated composite face sheets

was also investigated on the natural frequency of FG nanocomposite shells in (Tornabene *et al.* 2016). The buckling response of plates and panels made of CNTs reinforced nanocomposite was investigated using FE shell method in (Zghal *et al.* 2018). Trabelsi *et al.* (2019) presented thermal buckling analysis of CNT reinforced nanocomposite plates and shells using FE shell method and a modified FSDT. The buckling analysis of composite laminated plates has been conducted using a FSDT and HSDT based a meshless method in Zarei and Khosravifard (2019). For hexagonal plates, Ghanati and Safaei (2019) employed an energy method based on classical plate theory to conduct their buckling behavior.

Moreover, the buckling analysis of different sandwich structures have been reported. Pandit *et al.* (2008) suggested a sandwich plates with two laminated composite face sheets and a soft core and conducted their buckling behaviors using an isotropic FEM. Ćetković and Vuksanović (2009) considered the same sandwich plates but with honeycomb or isotropic cores and presented their mechanical behaviors using FEM based on layerwise displacement model. Nguyen *et al.* (2015) proposed a sandwich plate with a homogeneous core and two FGM face sheets and presented their mechanical behaviors using Navier and FE methods and a four-unknown RSDT. Considering circular sandwich plates with a tapered core and FG nanocomposite face sheets reinforced with CNT, Jalali and Heshmati (2016) reported buckling behavior using shooting method. Shokravi (2017) proposed sandwich plates including one orthotropic elastic core and FG nanocomposite layers subjected to magnetic fields and presented their buckling behaviors using Navier's method and HSDT. Adopting the same method, Moradi-Dastjerdi and Malek-Mohammadi (2017b) presented biaxial buckling behaviors of sandwich plates with laminated composites core and FG nanocomposite face sheets reinforced with CNT agglomerations. The improvement of buckling behavior laminated sandwich panels due to the use of shape memory alloy fibers has been studied by (Katariya *et al.* 2017).

In order to reduce the structural weight or control the performance of structures, porosities can be created inside some engineering structures (Safaei *et al.* 2019a, Tang *et al.* 2018). The buckling behavior of different porous structures

has been reported. Jabbari *et al.* (2013) analytically presented the nonlinear buckling behavior of FGP circular plates integrated with piezoelectric layers. Also, nonlinear thermal buckling, and mechanical buckling and postbuckling behaviors of saturated FGP circular plates have been presented in (Feyzi and Khorshidvand 2017, Jabbari *et al.* 2014, Mojahedin *et al.* 2016). Karami *et al.* (2018) presented the effect of evenly dispersed pores on the critical buckling temperature of porous FG nanobeams integrated with piezoelectric layers using HSDT beam theory and Hamilton's principle. Shafiei and Kazemi (2017) proposed a porous tapered Euler-Bernoulli micro and nanobeams made of 2D-FGMs and evaluated their buckling behavior using generalized DQ method. Guessas *et al.* (2018) suggested porous plates made of FG CNT-reinforced nanocomposites and presented their buckling behavior using an FSDT based analytical approach.

The successful application of FGM concept and foams in different industries, and the significance of designing lightweight structures have been motivated this paper to propose sandwich plates consisting of FGP cores and laminated composite face sheets. Particularly, this paper presents the buckling behavior of the proposed PSPs resting on elastic foundation subjected to in-plane compression loads. Using FEM and FSDT, the effects of porosity distribution and volume, the number and angles of laminated layers, sandwich plate geometrical dimensions, elastic foundation coefficients, loading and boundary conditions have been evaluated.

2. Modeling of porous sandwich plate

As shown in Fig. 1, the considered sandwich plates include one porous core with two laminated composite face sheets located on elastic foundations with normal k_w and shear k_s coefficients. The proposed PSPs with length a , width b , face sheet thickness h_f , core thickness h_c and total thickness h , are assumed to be under in-plane buckling loads F_x and F_y . It is worth noting that $F_y = 0$ and $F_x = F_y$ represent uniaxial and biaxial buckling problems, respectively.

Moreover, three different patterns are considered for the distributions of porosities including uniform distributed

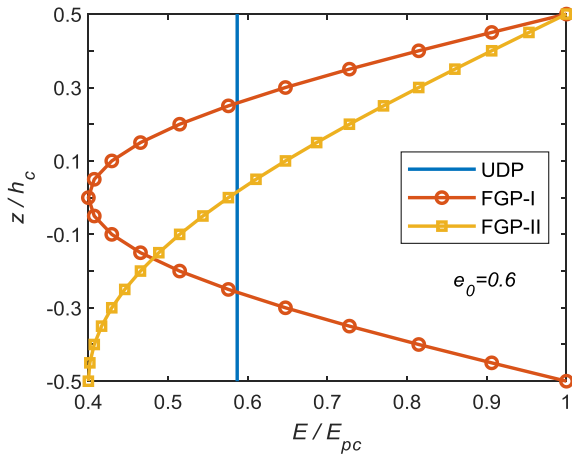


Fig. 2 The ratio of E/E_{pc} along the thickness of FGP core

porosity (UDP) and two types of FG distributions called FGP-I and FGP-II. In core, the Young's modulus ratio of porous to perfect materials (E/E_{pc}) can be evaluated as (Mojahedin *et al.* 2016)

$$\text{UDP: } E/E_{pc} = 1 - e_0 \zeta, \quad \zeta = \frac{1}{e_0} - \frac{1}{e_0} \left(\frac{2}{\pi} \sqrt{1 - e_0} - \frac{2}{\pi} + 1 \right)^2 \quad (1)$$

$$\text{FGP-I: } E/E_{pc} = 1 - e_0 \cos(\pi z/h_c) \quad (2)$$

$$\text{FGP-II: } E/E_{pc} = 1 - e_0 \cos\left(\frac{\pi z}{4h_c} + \frac{\pi}{4}\right) \quad (3)$$

where E , E_{pc} and e_0 are Young's modulus of porous core, Young's modulus of perfect (without porosity) core and porosity coefficient, respectively. The same equations have been also utilized for the shear modulus ratio of porous cores (G/G_{pc}). Fig. 2 illustrates the variation of E/E_{pc} along the thickness of FGP cores.

3. Governing equations of porous sandwich plate

3.1 Basic equations

In plates subjected to in-plane buckling loads, total energy function Π includes potential energy caused by in-plane forces W_g and strain energy U_ε and can be presented as (Tran *et al.* 2013)

$$\Pi = U_\varepsilon - W_g \quad (4)$$

where

$$U_\varepsilon = \frac{1}{2} \int_V [\boldsymbol{\varepsilon}_b^T \boldsymbol{\sigma} + \boldsymbol{\gamma}^T \boldsymbol{\tau}] dV + \frac{1}{2} \int_A [k_w w^2 + k_s \left[(\partial w / \partial x)^2 + (\partial w / \partial y)^2 \right]] dA \quad (5)$$

$$W_g = \frac{1}{2} \int_A \begin{bmatrix} \partial w / \partial x & \partial w / \partial y \end{bmatrix} \begin{bmatrix} F_x & 0 \\ 0 & F_y \end{bmatrix} \begin{bmatrix} \partial w / \partial x \\ \partial w / \partial y \end{bmatrix} dV \quad (6)$$

where V is the total volume of sandwich plate and A is a part of volume contacted to elastic foundation. $\boldsymbol{\varepsilon}_b$, $\boldsymbol{\gamma}$, $\boldsymbol{\sigma}$ and $\boldsymbol{\tau}$ are the vectors of in-plane strain, out of plane strain, in-plane stress and out of plane stress, respectively.

In the literature, different plate theories have been proposed to transform 3D solutions into 2D ones which result in a considerable reduction in computational cost. Based on the adopted FSDT in this work which has a good accuracy for thin and moderately thick plates, the displacement field of the proposed PSPs along x , y and z directions (u , v and w) can be defined as (Reddy 2004)

$$\begin{aligned} u(x, y, z) &= u_0(x, y) + z\theta_x(x, y) \\ v(x, y, z) &= v_0(x, y) + z\theta_y(x, y) \\ w(x, y, z) &= w_0(x, y) \end{aligned} \quad (7)$$

where u_0 , v_0 and w_0 are mid-plane displacements, and θ_x and θ_y represent transverse normal rotations around y - and x -axes, respectively. According to the definition of displacement field, in-plane and out of plane strain vectors can be expressed as (Reddy 2004)

$$\begin{aligned} \boldsymbol{\varepsilon}_b &= \left\{ \varepsilon_{xx} \quad \varepsilon_{yy} \quad \gamma_{xy} \right\}^T = \boldsymbol{\varepsilon}_0 + z\boldsymbol{\varepsilon}_1, \\ \boldsymbol{\gamma} &= \left\{ \gamma_{xz} \quad \gamma_{yz} \right\}^T \end{aligned} \quad (8)$$

where

$$\begin{aligned} \boldsymbol{\varepsilon}_0 &= \begin{Bmatrix} u_{0,x} \\ v_{0,y} \\ u_{0,y} + v_{0,x} \end{Bmatrix}, \boldsymbol{\varepsilon}_1 = \begin{Bmatrix} \theta_{x,x} \\ \theta_{y,y} \\ \theta_{x,y} + \theta_{y,x} \end{Bmatrix}, \\ \boldsymbol{\gamma} &= \begin{Bmatrix} \theta_x + w_{0,x} \\ \theta_y + w_{0,y} \end{Bmatrix} \end{aligned} \quad (9)$$

In addition to strain vector, the stress vector and the constitutive law of PSP can be divided as follows (Reddy 2004)

$$\begin{aligned} \begin{Bmatrix} \sigma_x \\ \sigma_y \\ \sigma_{xy} \end{Bmatrix} &= \begin{bmatrix} Q_{11} & Q_{12} & Q_{16} \\ Q_{12} & Q_{22} & Q_{26} \\ Q_{26} & Q_{26} & Q_{66} \end{bmatrix} \begin{Bmatrix} \varepsilon_x \\ \varepsilon_y \\ \gamma_{xy} \end{Bmatrix} \text{ or } \boldsymbol{\sigma} = \mathbf{Q}_b \boldsymbol{\varepsilon}_b \\ \begin{Bmatrix} \sigma_{xz} \\ \sigma_{yz} \end{Bmatrix} &= \alpha \begin{bmatrix} Q_{55} & Q_{45} \\ Q_{45} & Q_{44} \end{bmatrix} \begin{Bmatrix} \gamma_{xz} \\ \gamma_{yz} \end{Bmatrix} \text{ or } \boldsymbol{\tau} = \frac{5}{6} \mathbf{Q}_s \boldsymbol{\gamma} \end{aligned} \quad (10)$$

where Q_{ij} are the components of elastic constant matrix of each layer which is location dependent for FGP core and fiber orientation dependent for laminated layers. These components for the isotropic porous core are defined as

$$\begin{aligned} Q_{11} &= Q_{22} = \frac{E(z)}{1 - \nu^2(z)}, Q_{12} = \nu Q_{11}, \\ Q_{44} &= Q_{55} = Q_{66} = G, Q_{16} = Q_{26} = Q_{45} = 0 \end{aligned} \quad (11)$$

where ν is Poisson's ratio. For each layers of laminated composite, Q_{ij} are also evaluated as

$$\begin{aligned} Q_{ij} &= \bar{C}_{ij} - (\bar{C}_{i3} \cdot \bar{C}_{ij}) / C_{33} \quad i, j = 1, 2, 6 \\ Q_{ij} &= \bar{C}_{ij} \quad i, j = 4, 5 \end{aligned} \quad (12)$$

where C_{ij} ($i, j = 1, 2, \dots, 6$) are the components of elastic constant matrix for a transverse isotropic materials. By considering θ as the orientation of fiber in each layers of laminated composite and by the definitions of $m = \cos \theta$ and $n = \sin \theta$, \bar{C}_{ij} could also be calculated as (Reddy 2004)

$$\begin{aligned} \bar{C}_{11} &= m^4 C_{11} + 2m^2 n^2 (C_{12} + 2C_{66}) + n^4 C_{22}, \\ \bar{C}_{22} &= n^4 C_{11} + 2m^2 n^2 (C_{12} + 2C_{66}) + m^4 C_{22}, \\ \bar{C}_{12} &= m^2 n^2 (C_{11} + C_{22} + 4C_{66}) + (m^4 + n^4) C_{12}, \\ \bar{C}_{66} &= -m^2 n^2 (C_{11} + C_{22} - 2C_{12}) + (m^4 - n^4) C_{66}, \\ \bar{C}_{16} &= -mn [n^2 C_{11} - m^2 C_{22} - (m^2 - n^2)(C_{12} + 2C_{66})] \\ \bar{C}_{26} &= -mn [m^2 C_{11} - n^2 C_{22} - (m^2 - n^2)(C_{12} + 2C_{66})] \\ \bar{C}_{13} &= m^2 C_{13} + n^2 C_{23}, \quad \bar{C}_{23} = n^2 C_{13} + m^2 C_{23}, \\ \bar{C}_{36} &= (C_{32} - C_{31})nm, \quad \bar{C}_{44} = m^2 C_{44} + n^2 C_{55}, \\ \bar{C}_{55} &= m^2 C_{55} + n^2 C_{44}, \quad \bar{C}_{45} = (C_{45} - C_{55})nm \end{aligned} \quad (13)$$

3.2 FEM formulation

The displacement of PSP can be estimated using a combination of first order theory and FEM. In FEM, displacement field \mathbf{U} is evaluated at some predefined nodes called nodal values as follows (Moradi-Dastjerdi and Momeni-Khabisi 2016)

$$\mathbf{U} = [u_{0i}, v_{0i}, w_{0i}, \theta_{xi}, \theta_{yi}]^T = \sum_{i=1}^n N_i U_i \quad (14)$$

where N_i are the values of utilized bilinear rectangular shape functions at each node. It should be mentioned that the selected four-node element is easy to define and causes low computational costs. Introducing Eq. (14) into Eq. (8) leads to following definition of strain vectors at predefined nodes (Safaei *et al.* 2019b)

$$\boldsymbol{\varepsilon}_b = \{\mathbf{B}_0 + z \mathbf{B}_1\} \mathbf{U}, \quad \boldsymbol{\gamma} = \mathbf{B}_s \mathbf{U} \quad (15)$$

where

$$\mathbf{B}_0 = \begin{bmatrix} N_{i,x} & 0 & 0 & 0 & 0 \\ 0 & N_{i,y} & 0 & 0 & 0 \\ N_{i,y} & N_{i,x} & 0 & 0 & 0 \end{bmatrix}, \quad (16)$$

$$\begin{aligned} \mathbf{B}_1 &= \begin{bmatrix} 0 & 0 & 0 & N_{i,x} & 0 \\ 0 & 0 & 0 & 0 & N_{i,y} \\ 0 & 0 & 0 & N_{i,y} & N_{i,x} \end{bmatrix}, \\ \mathbf{B}_s &= \begin{bmatrix} 0 & 0 & N_{i,x} & N_i & 0 \\ 0 & 0 & N_{i,y} & 0 & N_i \end{bmatrix} \end{aligned} \quad (16)$$

Introducing Eqs. (5), (6), (10) and (15) into the total energy function (Eq. (4)) results in

$$\begin{aligned} \Pi &= \frac{1}{2} \int_A \mathbf{U}^T \left\{ \begin{bmatrix} \mathbf{B}_0^T & \mathbf{B}_1^T \end{bmatrix} \bar{\mathbf{Q}}_b \begin{bmatrix} \mathbf{B}_0 & \mathbf{B}_1 \end{bmatrix}^T + \mathbf{B}_s^T \bar{\mathbf{Q}}_s \mathbf{B}_s + \mathbf{B}_p^T \mathbf{F}_b \mathbf{B}_p \right\} \mathbf{U} dA \\ &+ \frac{1}{2} \int_A \mathbf{U}^T \left[\mathbf{N}_w^T k_w \mathbf{N}_w + \mathbf{B}_p^T k_s \mathbf{B}_p \right] \mathbf{U} dA \end{aligned} \quad (17)$$

where

$$\begin{aligned} \bar{\mathbf{Q}}_b &= \int_{-h/2}^{h/2} \begin{bmatrix} 1 & z^2 \\ z^2 & z^4 \end{bmatrix} \mathbf{Q}_b dz, \\ \bar{\mathbf{Q}}_s &= \frac{5}{6} \int_{-h/2}^{h/2} \mathbf{Q}_s dz, \quad \mathbf{F}_b = \begin{bmatrix} F_x & 0 \\ 0 & F_y \end{bmatrix} \end{aligned} \quad (18)$$

$$\begin{aligned} \mathbf{N}_w &= [0 \quad 0 \quad N_i \quad 0 \quad 0], \\ \mathbf{B}_p &= \begin{bmatrix} 0 & 0 & N_{i,x} & 0 & 0 \\ 0 & 0 & N_{i,y} & 0 & 0 \end{bmatrix} \end{aligned} \quad (19)$$

By setting zero of the derivation of Eq. (17) with respect to nodal values of displacement fields \mathbf{U} , the buckling eigenvalue equation of the proposed porous sandwich plates is defined as

$$(\mathbf{K} + F_{cr} \mathbf{K}_G) \mathbf{U} = 0 \quad (20)$$

where F_{cr} is the critical buckling value of PSPs. Also, \mathbf{K} is stiffness matrix and \mathbf{K}_G is geometrical stiffness matrix which are given by

$$\begin{aligned} \mathbf{K} &= \int_A \left\{ \begin{bmatrix} \mathbf{B}_0^T & \mathbf{B}_1^T \end{bmatrix} \bar{\mathbf{Q}}_b \begin{bmatrix} \mathbf{B}_0 & \mathbf{B}_1 \end{bmatrix}^T + \mathbf{B}_s^T \bar{\mathbf{Q}}_s \mathbf{B}_s \right\} dA \\ &+ \int_A \left[\mathbf{N}_w^T k_w \mathbf{N}_w + \mathbf{B}_p^T k_s \mathbf{B}_p \right] dA \end{aligned} \quad (21)$$

$$\mathbf{K}_G = \int_A \mathbf{B}_p^T \mathbf{F}_b \mathbf{B}_p dA \quad (22)$$

4. Results and discussions

The following normalized parameters have been utilized through the present paper

$$\begin{aligned} \bar{F}_{cr} &= F_{cr} a^2 / D, \quad K_w = k_w a^4 / D, \\ K_s &= k_s a^2 / D \quad \text{and} \quad D = Eh^3 / 12(1 - \nu^2) \end{aligned} \quad (23)$$

Table 1 Comparison of the first four uniaxial \bar{F}_{cr} for the considered isotropic plate

Mode	Present FEM	Analytical (Timoshenko and Gere 1961)	Numerical (Zhao <i>et al.</i> 2009)
1 st	39.5499	39.4761	39.2040
2 nd	62.0989	61.6814	60.396
3 rd	111.7337	109.656	103.963
4 th	159.0604	157.904	151.987

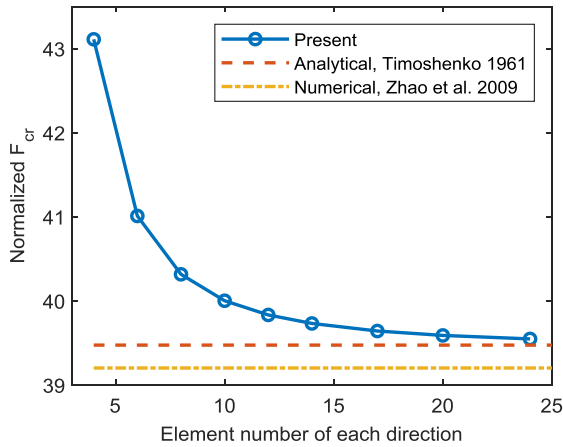


Fig. 3 The convergence of first uniaxial \bar{F}_{cr} for the considered isotropic plate

4.1 Validation of models

In order to examine the accuracy and convergence of the developed FEM, the obtained uniaxial critical buckling loads \bar{F}_{cr} have been compared with those obtained from analytical (Timoshenko and Gere 1961) and numerical (Zhao *et al.* 2009) methods. Table 1 shows this comparison for the first four buckling loads of simply supported isotropic plates with $a = b = 10$ in, $h = 0.1$ in, $E = 3 \times 10^6$ psi

and $\nu = 0.316$. Very good agreements with analytical results, even better than the other numerical method (Zhao *et al.* 2009), are observed for all four modes. In addition to the accuracy of the developed method, its convergence for the first buckling load of the same plates has been examined in Fig. 3. It can be seen that the developed method has a very good convergence as well such that the use of few numbers of elements along each direction leads to very accurate buckling loads. Fig. 3 shows that the use of 17 elements in each direction results in a very good accuracy. Therefore, we utilized 17×17 elements for the following simulations.

4.2 Buckling loads of porous sandwich plates

In the modelling of PSPs, unless otherwise specified, simply supported square PSPs including an FGP-I core and two laminated composite face sheets with a symmetric stacking sequence of $[45, -45, 45, -45]$ with $h_c/a = 0.01$, $h_f/h_c = 0.1$ and without elastic foundation $K_w = K_s = 0$ have been considered. FGP core and laminated composite face sheets are assumed to be made of Epoxy with $E_{pc} = 4.5$ GPa, $\nu_{pc} = 0.4$ and Graphite/Epoxy (Gr/Ep) with $E_{11} = 132.38$ GPa, $E_{12} = E_{13} = 10.756$ GPa, $\nu_{12} = \nu_{13} = 0.24$, $\nu_{23} = 0.49$, respectively (Dash and Singh 2009). It should also be mentioned that the normalized critical buckling loads \bar{F}_{cr} of PSPs are calculated based on the material properties of perfect Epoxy (core). Moreover, S, C and F have been utilized for PSPs' edge constrains which are simply supported, clamped and free, respectively.

Fig. 4 shows the effect of porosity volume and distribution types on the uniaxial and biaxial critical buckling load parameters \bar{F}_{cr} of PSPs. It can be seen that the increase of porosity parameter e_0 results in a similar reduction in uniaxial and biaxial buckling loads of PSPs. The maximum reduction in buckling loads is observed for the considered PSPs with UDP cores which is less than 9%. The substitution of UDP core with FGP cores results in a better buckling behavior such that critical buckling loads show only 5% reduction. Therefore, it can be seen that the use of FGP core can offer a PSP with half weight core and only 5% reduction in critical buckling loads.

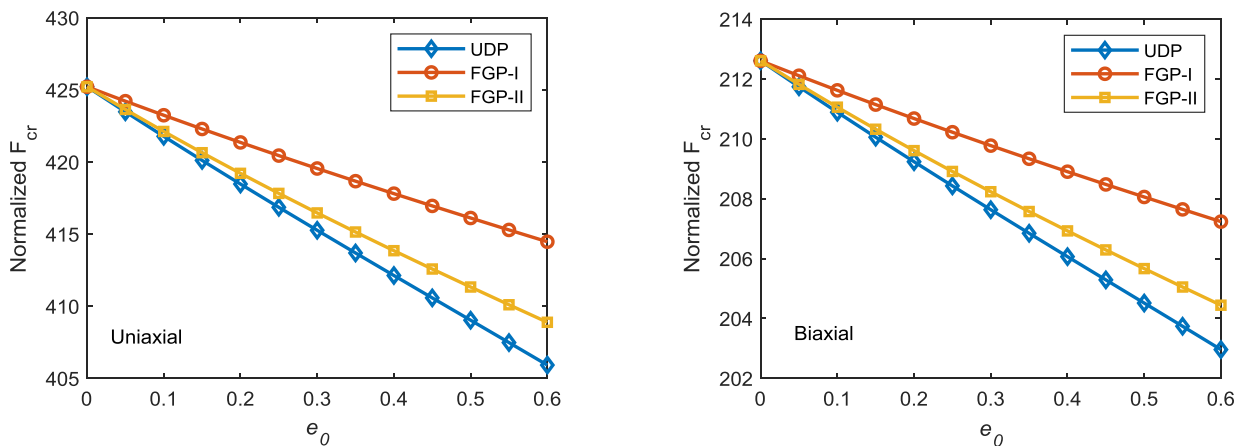


Fig. 4 (a) Uniaxial; (b) biaxial \bar{F}_{cr} as a function of porosity parameter for SSSS square PSPs with different porous cores and with $h_c/a = 0.01$, $h_f/h_c = 0.1$, $K_w = K_s = 0$ and $[45, -45, 45, -45]$

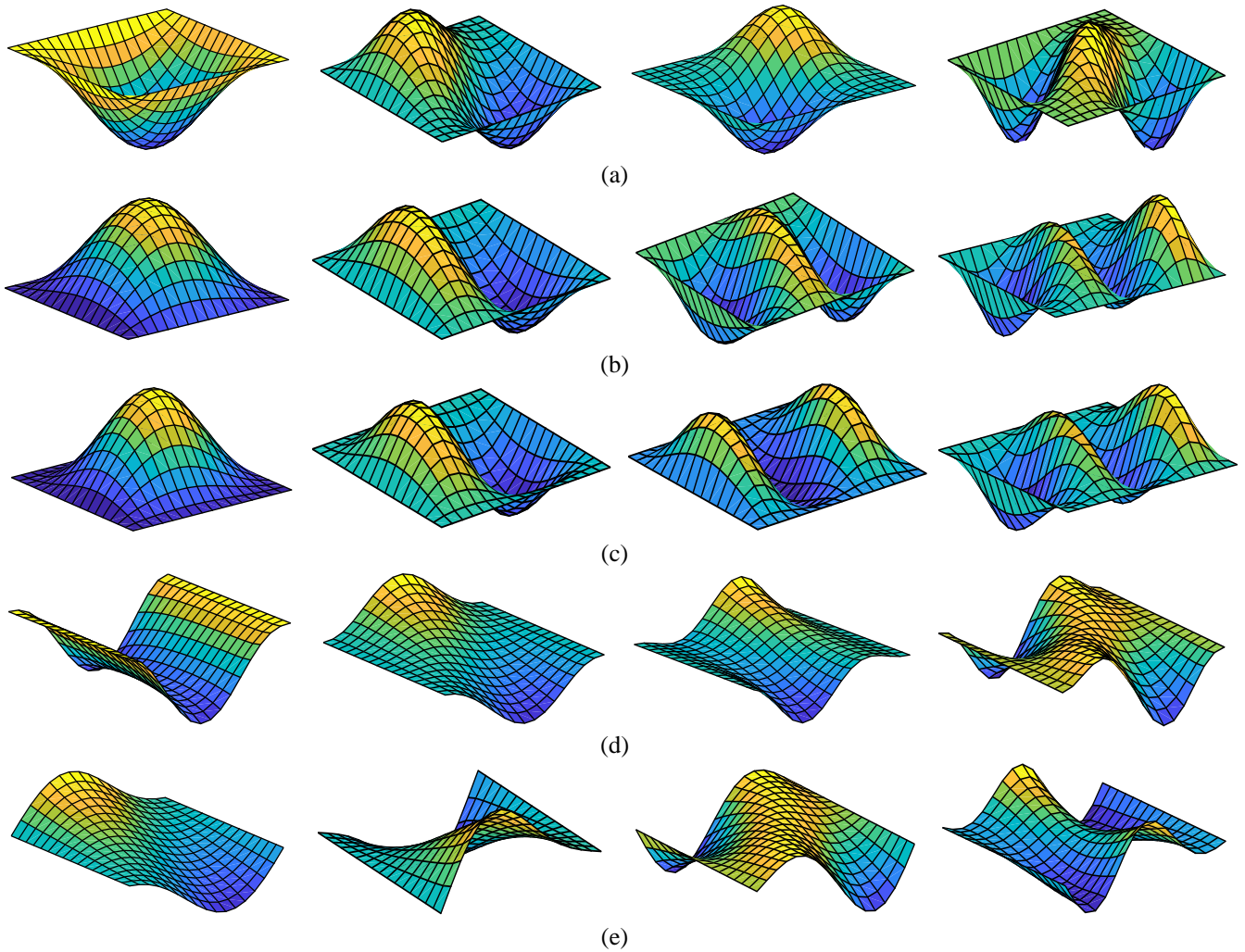


Fig. 5 First four mode shapes of square [45, -45, 45, -45] PSPs with (a) SSSS, uniaxial (b) SSSS, biaxial (c) CSCS, uniaxial (d) CFCF, uniaxial (e) SFSE, uniaxial

Table 2 Biaxial \bar{F}_{cr} for SSSS square PSPs with different cores and stacking sequence of laminated composites with $h_c/a = 0.01$, $h_f/h_c = 0.1$ and $K_w = K_s = 0$

	Perfect $e_0 = 0$	UDP $e_0 = 0.6$	FGP-I $e_0 = 0.6$	FGP-II $e_0 = 0.6$
[0, 90]	135.25	125.72	130.00	127.08
[45, -45]	212.28	202.61	206.90	204.10
[30, -30]	192.98	183.33	187.62	184.75
[0, 45, 90]	154.03	144.03	148.52	145.48
[45, 0, -45]	186.59	176.96	181.24	178.40
[30, 0, -30]	173.68	164.06	168.34	165.42
[0, 30, 60, 90]	152.42	142.09	146.73	143.57
[45, -45, 45, -45]	212.61	202.96	207.23	204.44
[0, 90, 0, 90]	135.25	125.72	130.00	127.09
[0, 30, 45, 60, 90]	155.39	144.62	149.47	146.14
[90, 60, 45, 30, 0]	155.39	144.62	149.47	146.14
[45, -45, 45, -45, 45]	210.56	200.81	205.13	202.30
[30, -30, 30, -30, 30]	191.63	181.91	186.23	183.34

The effects of fibre orientation and the number of plies on the biaxial \bar{F}_{cr} of PSP are presented in Table 2 for perfect and porous cores. Maximum and minimum buckling parameters are observed for laminated composites with fibre orientations of ± 45 and $0/90$ degrees, respectively. It can be seen that fibre orientation can sharply improve buckling load parameters from 117.86 to 180.74, although the number of plies does not have a significant effect. In all cases, the critical buckling loads of PSPs with FGP cores are much higher than those with UDP core.

The effect of PSPs' edge constrains on the first four uniaxial and biaxial buckling loads \bar{F}_{cr} of PSPs with perfect and FGP-I cores are presented in Table 3. As expected, PSPs with more constrains have higher values of \bar{F}_{cr} . Also, the use of FGP-I core, which is very lighter than perfect core, results in only about 7% reduction in almost all cases of PSPs. Fig. 5 illustrates the effects of edges constrains and buckling loading conditions of PSPs on the first four mode shapes of buckling responses. It is observed that these two parameters can totally change the buckling mode shapes of PSPs.

Table 3 Uniaxial and biaxial \bar{F}_{cr} of square PSPs with different boundary conditions and with $h_c/a = 0.01$, $h_f/h_c = 0.1$, $K_w = K_s = 0$ and [45, -45, 45, -45]

B.C.	Mode	Uniaxial		Biaxial	
		Perfect $e_0 = 0$	FGP-I $e_0 = 0.6$	Perfect $e_0 = 0$	FGP-I $e_0 = 0.6$
CSCS	1 st	695.18	672.66	346.066	335.38
	2 nd	767.85	743.63	541.94	524.65
	3 rd	990.85	954.29	725.85	700.27
	4 th	1494.71	1433.15	885.48	853.05
FCFC	1 st	250.79	240.74	225.13	216.93
	2 nd	480.72	466.84	229.98	223.42
	3 rd	533.66	511.64	329.01	318.41
	4 th	753.37	727.03	505.16	484.81
SSSS	1 st	425.21	414.47	212.61	207.23
	2 nd	579.33	561.81	459.24	445.22
	3 rd	925.78	892.64	469.60	455.53
	4 th	1451.82	1393.13	828.14	799.56
FSFS	1 st	54.44	52.31	52.21	50.21
	2 nd	243.56	233.85	127.57	125.19
	3 rd	293.39	287.79	235.68	226.40
	4 th	473.99	460.33	246.94	240.74

Fig. 6 shows the effects of geometrical dimensions on the uniaxial and biaxial \bar{F}_{cr} of PSPs with perfect cores. As shown in Fig. 6(a), both uniaxial and biaxial \bar{F}_{cr} are significantly increased by the increase of face sheet thicknesses. The reason is the elasticity moduli of Gr/Ep (outer layers material) are much higher than that of Epoxy (core material). Moreover, the increase of h_f increases the moment of inertia and the resultant moment along PSP's thickness. Furthermore, Fig. 6(b) shows that the increase of b/a dramatically decreases both uniaxial and biaxial \bar{F}_{cr} of PSPs. Because by the increase of this ratio, the plate is

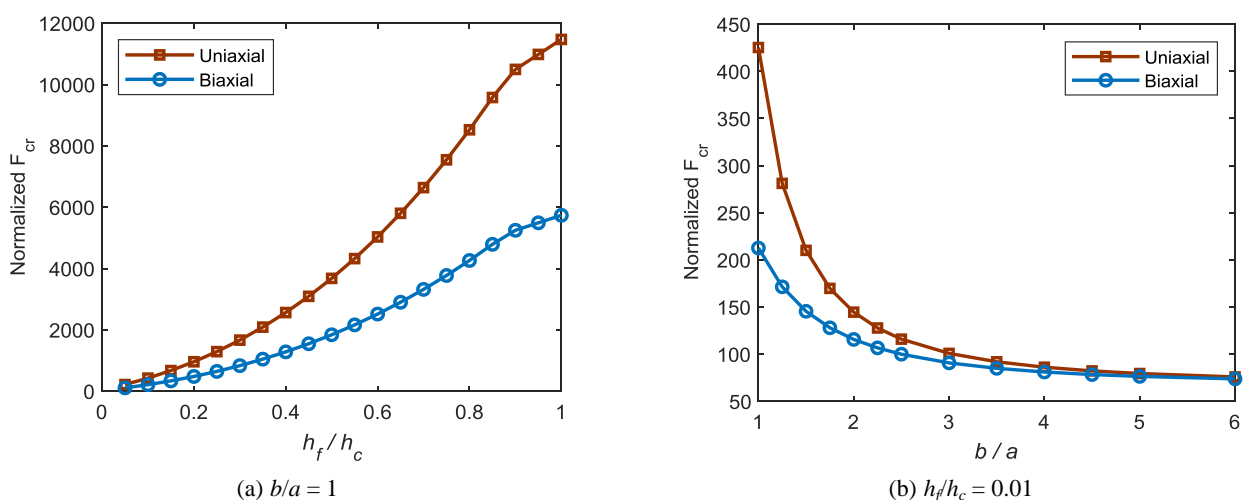


Fig. 6 Uniaxial and biaxial \bar{F}_{cr} as a function of (a) h_f/h_c ; (b) b/a for simply supported PSPs with perfect core $h_c/a = 0.01$, $K_w = K_s = 0$ and [45, -45, 45, -45]

transformed into a beam and it is already well established that beams have much less stiffness than plates.

Finally, the effects of shear and normal coefficients of elastic foundation on the uniaxial and biaxial buckling parameters of PSPs with perfect core are plotted in Fig. 7. It can be seen that for the considered ranges of K_w and K_s , the increase of each coefficient linearly improves the \bar{F}_{cr} of the considered PSPs. However, the effect of shear coefficient is much stronger than that of normal one.

5. Conclusions

This paper presented the buckling behavior of lightweight porous sandwich plates with FGP cores and laminated composite face sheets. The proposed PSPs were assumed to be under in-plane compression loads and rested on elastic foundations. According to the adopted FSDT and using FEM, governing equations were discretized, and the following results were obtained from the simulations of the proposed PSPs:

- Increase of porosity parameter decreases critical buckling loads.
- The use of FGP cores shows better buckling responses than UDP ones.
- The highest values of buckling loads are observed when stacking sequences only include fibers with ± 45 orientations.
- The number of plies does not have a significant effect on buckling behavior

References

- Afsharmanesh, B., Ghaheri, A. and Taheri-Behrooz, F. (2014), "Buckling and vibration of laminated composite circular plate on Winkler-type foundation", *Steel Compos. Struct., Int. J.*, **17**(1), 1-19. <https://doi.org/10.12989/scs.2014.17.1.001>
- Aram, E. and Mehdipour-Ataei, S. (2016), "A review on the micro- and nanoporous polymeric foams: Preparation and properties", *Int. J. Polym. Mater. Polym. Biomater.*, **65**, 358-

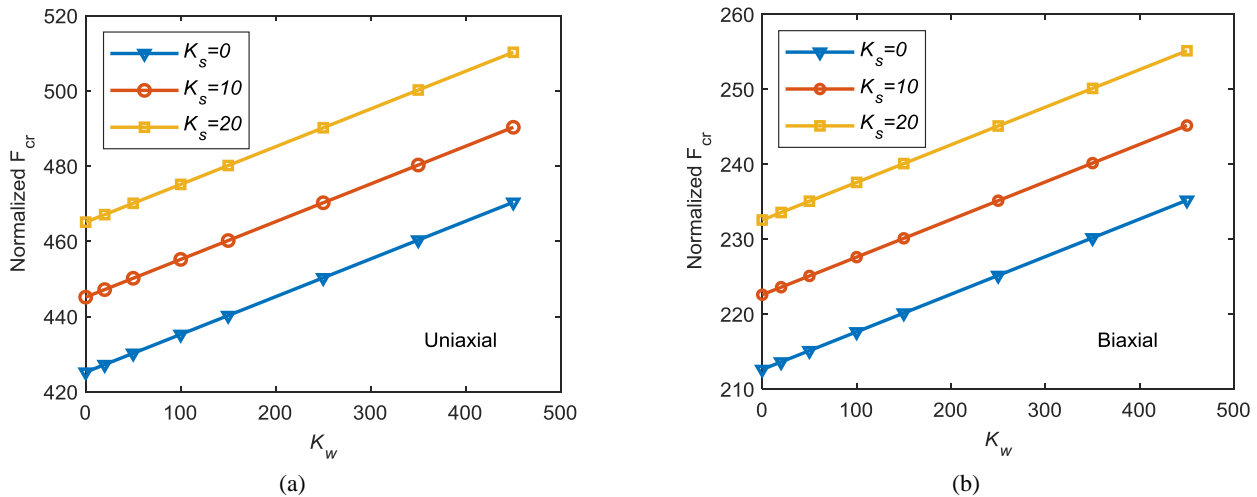


Fig. 7 (a) Uniaxial (b) biaxial \bar{F}_{cr} as a function of K_w for SSSS square PSPs with perfect core and with $h_c/a = 0.01$, $h_f/h_c = 0.1$ and $[45, -45, 45, -45]$

375. <https://doi.org/10.1080/00914037.2015.1129948>
- Birman, V. and Kardomateas, G.A. (2018), "Review of current trends in research and applications of sandwich structures", *Compos. Part B Eng.*, **142**, 221-240. <https://doi.org/10.1016/j.compositesb.2018.01.027>
- Ćetković, M. and Vuksanović, D. (2009), "Bending, free vibrations and buckling of laminated composite and sandwich plates using a layerwise displacement model", *Compos. Struct.*, **88**, 219-227. <https://doi.org/10.1016/j.compstruct.2008.03.039>
- Dash, P. and Singh, B.N. (2009), "Nonlinear free vibration of piezoelectric laminated composite plate", *Finite Elem. Anal. Des.*, **45**, 686-694. <https://doi.org/10.1016/j.finell.2009.05.004>
- Dehghan, M. and Baradaran, G.H. (2011), "Buckling and free vibration analysis of thick rectangular plates resting on elastic foundation using mixed finite element and differential quadrature method", *Appl. Math. Comput.*, **218**, 2772-2784. <https://doi.org/10.1016/j.amc.2011.08.020>
- Fattahi, A.M. and Safaei, B. (2017), "Buckling analysis of CNT-reinforced beams with arbitrary boundary conditions", *Microsyst. Technol.*, **23**, 5079-5091. <https://doi.org/10.1007/s00542-017-3345-5>
- Feyzi, M.R. and Khorshidvand, A.R. (2017), "Axisymmetric post-buckling behavior of saturated porous circular plates", *Thin Wall. Struct.*, **112**, 149-158. <https://doi.org/10.1016/j.tws.2016.11.026>
- Frikha, A., Zghal, S. and Dammak, F. (2018), "Dynamic analysis of functionally graded carbon nanotubes-reinforced plate and shell structures using a double directors finite shell element", *Aerosp. Sci. Technol.*, **78**, 438-451. <https://doi.org/10.1016/j.ast.2018.04.048>
- Ghanati, P. and Safaei, B. (2019), "Elastic buckling analysis of polygonal thin sheets under compression", *Indian J. Phys.*, **93**, 47-52. <https://doi.org/10.1007/s12648-018-1254-9>
- Guessas, H., Zidour, M., Meradjah, M., Tounsi, A. (2018), "The critical buckling load of reinforced nanocomposite porous plates", *Struct. Eng. Mech., Int. J.*, **67**(2), 115-123. <https://doi.org/10.12989/sem.2018.67.2.115>
- Jabbari, M., Joubaneh, E.F., Khorshidvand, A.R. and Eslami, M.R. (2013), "Buckling analysis of porous circular plate with piezoelectric actuator layers under uniform radial compression", *Int. J. Mech. Sci.*, **70**, 50-56. <https://doi.org/10.1016/j.ijmecsci.2013.01.031>
- Jabbari, M., Hashemitaheeri, M., Mojahedin, A. and Eslami, M.R. (2014), "Thermal buckling analysis of functionally graded thin circular plate made of saturated porous materials", *J. Therm. Stress.*, **37**, 202-220. <https://doi.org/10.1080/01495739.2013.839768>
- Jalali, S.K. and Heshmati, M. (2016), "Buckling analysis of circular sandwich plates with tapered cores and functionally graded carbon nanotubes-reinforced composite face sheets", *Thin-Wall. Struct.*, **100**, 14-24. <https://doi.org/10.1016/j.tws.2015.12.001>
- Karami, B., Shahsavari, D., Nazemosadat, S.M.R., Li, L. and Ebrahimi, A. (2018), "Thermal buckling of smart porous functionally graded nanobeam rested on Kerr foundation", *Steel Compos. Struct., Int. J.*, **29**(3), 349-362. <https://doi.org/10.12989/scs.2018.29.3.349>
- Katariya, P.V., Panda, S.K., Hirwani, C.K., Mehar, K. and Thakare, O. (2017), "Enhancement of thermal buckling strength of laminated sandwich composite panel structure embedded with shape memory alloy fibre", *Smart Struct. Syst., Int. J.*, **20**(5), 595-605. <https://doi.org/10.12989/sss.2017.20.5.595>
- Malekzadeh, P. and Karami, G. (2008), "A mixed differential quadrature and finite element free vibration and buckling analysis of thick beams on two-parameter elastic foundations", *Appl. Math. Model.*, **32**, 1381-1394. <https://doi.org/10.1016/j.apm.2007.04.019>
- Mojahedin, A., Jabbari, M., Khorshidvand, A.R. and Eslami, M.R. (2016), "Buckling analysis of functionally graded circular plates made of saturated porous materials based on higher order shear deformation theory", *Thin Wall. Struct.*, **99**, 83-90. <https://doi.org/10.1016/j.tws.2015.11.008>
- Moradi-Dastjerdi, R. and Malek-Mohammadi, H. (2017a), "Free vibration and buckling analyses of functionally graded nanocomposite plates reinforced by carbon nanotube", *Mech. Adv. Compos. Struct.*, **4**, 59-73. <https://doi.org/10.22075/MACS.2016.496>
- Moradi-Dastjerdi, R. and Malek-Mohammadi, H. (2017b), "Biaxial buckling analysis of functionally graded nanocomposite sandwich plates reinforced by aggregated carbon nanotube using improved high-order theory", *J. Sandw. Struct. Mater.*, **19**, 736-769. <https://doi.org/10.1177/1099636216643425>
- Moradi-Dastjerdi, R. and Momeni-Khabisi, H. (2016), "Dynamic analysis of functionally graded nanocomposite plates reinforced by wavy carbon nanotube", *Steel Compos. Struct., Int. J.*, **22**, 277-299. <https://doi.org/10.12989/scs.2016.22.2.277>
- Moradi-Dastjerdi, R. and Pourasghar, A. (2016), "Dynamic analysis of functionally graded nanocomposite cylinders reinforced by wavy carbon nanotube under an impact load", *J.*

- Vib. Control*, **22**, 1062-1075.
<https://doi.org/10.1177/1077546314539368>
- Nguyen, K., Thai, H.T. and Vo, T. (2015), "A refined higher-order shear deformation theory for bending, vibration and buckling analysis of functionally graded sandwich plates", *Steel Compos. Struct., Int. J.*, **18**(1), 91-120.
<https://doi.org/10.12989/scs.2015.18.1.091>
- Pandit, M.K., Singh, B.N. and Sheikh, A.H. (2008), "Buckling of laminated sandwich plates with soft core based on an improved higher order zigzag theory", *Thin-Wall. Struct.*, **46**, 1183-1191.
<https://doi.org/10.1016/j.tws.2008.03.002>
- Pourasghar, A. and Chen, Z. (2016), "Thermoelastic response of CNT reinforced cylindrical panel resting on elastic foundation using theory of elasticity", *Compos. Part B Eng.*, **99**, 436-444.
<https://doi.org/10.1016/j.compositesb.2016.06.028>
- Pourasghar, A. and Chen, Z. (2019a), "Effect of hyperbolic heat conduction on the linear and nonlinear vibration of CNT reinforced size-dependent functionally graded microbeams", *Int. J. Eng. Sci.*, **137**, 57-72.
<https://doi.org/10.1016/j.ijengsci.2019.02.002>
- Pourasghar, A. and Chen, Z. (2019b), "Hyperbolic heat conduction and thermoelastic solution of functionally graded CNT reinforced cylindrical panel subjected to heat pulse", *Int. J. Solids Struct.*, **163**, 117-129.
<https://doi.org/10.1016/j.ijsolstr.2018.12.030>
- Pourasghar, A. and Chen, Z. (2019c), "Nonlinear vibration and modal analysis of FG nanocomposite sandwich beams reinforced by aggregated CNTs", *Polym. Eng. Sci.*,
<https://doi.org/10.1002/pen.25119>
- Pourasghar, A. and Kamarian, S. (2015), "Dynamic stability analysis of functionally graded nanocomposite non-uniform column reinforced by carbon nanotube", *J. Vib. Control*, **21**, 2499-2508. <https://doi.org/10.1177/1077546313513625>
- Pourasghar, A., Moradi-Dastjerdi, R., Yas, M.H., Ghorbanpour Arani, A. and Kamarian, S. (2018), "Three-dimensional analysis of carbon nanotube-reinforced cylindrical shells with temperature-dependent properties under thermal environment", *Polym. Compos.*, **39**, 1161-1171.
<https://doi.org/10.1002/pc.24046>
- Reddy, J.N. (2004), *Mechanics of Laminated Composite Plates and Shells: Theory and Analysis*, CRC press.
- Shafiei, N. and Kazemi, M. (2017), "Buckling analysis on the bi-dimensional functionally graded porous tapered nano-/micro-scale beams", *Aerosp. Sci. Technol.*, **66**, 1-11.
<https://doi.org/10.1016/j.ast.2017.02.019>
- Shahsavari, D., Karami, B. and Li, L. (2018), "A high-order gradient model for wave propagation analysis of porous FG nanoplates", *Steel Compos. Struct., Int. J.*, **29**(1), 53-66.
<https://doi.org/10.12989/scs.2018.29.1.053>
- Safaei, B., Moradi-Dastjerdi, R., Behdinin, K. and Chu, F. (2019a), "Critical buckling temperature and force in porous sandwich plates with CNT-reinforced nanocomposite layers", *Aerosp. Sci. Technol.*, **91**, 175-185.
<https://doi.org/10.1016/j.ast.2019.05.020>
- Safaei, B., Moradi-Dastjerdi, R., Qin, Z. and Chu, F. (2019b), "Frequency-dependent forced vibration analysis of nano-composite sandwich plate under thermo-mechanical loads", *Compos. Part B Eng.*, **161**, 44-54.
<https://doi.org/10.1016/j.compositesb.2018.10.049>
- Shokravi, M. (2017), "Buckling of sandwich plates with FG-CNT-reinforced layers resting on orthotropic elastic medium using Reddy plate theory", *Steel Compos. Struct., Int. J.*, **23**(6), 623-631. <https://doi.org/10.12989/scs.2017.23.6.623>
- Shokri-Oojghaz, R., Moradi-Dastjerdi, R., Mohammadi, H. and Behdinin, K. (2019), "Stress distributions in nanocomposite sandwich cylinders reinforced by aggregated carbon nanotube", *Polym. Compos.*, **40**, E1918-E1927.
<https://doi.org/10.1002/pc.25206>
- Singh, S., Singh, J. and Shukla, K. (2013), "Buckling of laminated composite plates subjected to mechanical and thermal loads using meshless collocations", *J. Mech. Sci. Technol.*, **27**, 327-336. <https://doi.org/10.1007/s12206-012-1249-y>
- Tang, H., Li, L. and Hu, Y. (2018), "Buckling analysis of two-directionally porous beam", *Aerosp. Sci. Technol.*, **78**, 471-479.
<https://doi.org/10.1016/j.ast.2018.04.045>
- Timoshenko, S. and Gere, J. (1961), *Theory of Elastic Stability*, McGraw-Hill, New York, NY, USA.
- Topal, U. (2012), "Thermal buckling load optimization of laminated plates with different intermediate line supports", *Steel Compos. Struct., Int. J.*, **13**(3), 207-223.
<https://doi.org/10.12989/scs.2012.13.3.207>
- Tornabene, F. and Reddy, J.N. (2013), "FGM and Laminated Doubly-Curved and Degenerate Shells Resting on Nonlinear Elastic Foundations: A GDQ Solution for Static Analysis with a Posteriori Stress and Strain Recovery", *J. Indian Inst. Sci.*, **93**, 635-688.
- Tornabene, F., Methods, C., Mech, A. and Tornabene, F. (2009), "Free vibration analysis of functionally graded conical, cylindrical shell and annular plate structures with a four-parameter power-law distribution", *Comput. Methods Appl. Mech. Eng.*, **198**, 2911-2935.
<https://doi.org/10.1016/j.cma.2009.04.011>
- Tornabene, F., Liverani, A. and Caligiana, G. (2011), "FGM and laminated doubly curved shells and panels of revolution with a free-form meridian: A 2-D GDQ solution for free vibrations", *Int. J. Mech. Sci.*, **53**, 446-470.
<https://doi.org/10.1016/j.ijmecsci.2011.03.007>
- Tornabene, F., Fantuzzi, N., Viola, E. and Batra, R.C. (2015), "Stress and strain recovery for functionally graded free-form and doubly-curved sandwich shells using higher-order equivalent single layer theory", *Compos. Struct.*, **119**, 67-89.
<https://doi.org/10.1016/j.compstruct.2014.08.005>
- Tornabene, F., Fantuzzi, N., Baccocchi, M. and Viola, E. (2016), "Effect of agglomeration on the natural frequencies of functionally graded carbon nanotube-reinforced laminated composite doubly-curved shells", *Compos. Part B Eng.*, **89**, 187-218. <https://doi.org/10.1016/j.compositesb.2015.11.016>
- Trabelsi, S., Frikha, A., Zghal, S. and Dammak, F. (2019), "A modified FSDT-based four nodes finite shell element for thermal buckling analysis of functionally graded plates and cylindrical shells", *Eng. Struct.*, **178**, 444-459.
<https://doi.org/10.1016/j.engstruct.2018.10.047>
- Tran, L.V., Thai, C.H. and Nguyen-Xuan, H. (2013), "An isogeometric finite element formulation for thermal buckling analysis of functionally graded plates", *Finite Elem. Anal. Des.*, **73**, 65-76. <https://doi.org/10.1016/j.finela.2013.05.003>
- Yu, T., Yin, S., Bui, T.Q., Xia, S., Tanaka, S. and Hirose, S. (2016), "NURBS-based isogeometric analysis of buckling and free vibration problems for laminated composites plates with complicated cutouts using a new simple FSDT theory and level set method", *Thin Wall. Struct.*, **101**, 141-156.
<https://doi.org/10.1016/j.tws.2015.12.008>
- Zarei, A. and Khosravifard, A. (2019), "A meshfree method for static and buckling analysis of shear deformable composite laminates considering continuity of interlaminar transverse shearing stresses", *Compos. Struct.*, **209**, 206-218.
<https://doi.org/10.1016/j.compstruct.2018.10.077>
- Zghal, S., Frikha, A. and Dammak, F. (2018), "Mechanical buckling analysis of functionally graded power-based and carbon nanotubes-reinforced composite plates and curved panels", *Compos. Part B Eng.*, **150**, 165-183.
<https://doi.org/10.1016/j.compositesb.2018.05.037>
- Zhang, L.W., Lei, Z.X. and Liew, K.M. (2015), "Buckling analysis of FG-CNT reinforced composite thick skew plates using an

element-free approach”, *Compos. Part B Eng.*, **75**, 36-46.

<https://doi.org/10.1016/j.compositesb.2015.01.033>

Zhao, X., Lee, Y.Y. and Liew, K.M. (2009), “Mechanical and thermal buckling analysis of functionally graded plates”, *Compos. Struct.*, **90**, 161-171.

<https://doi.org/10.1016/j.compstruct.2009.03.005>

CC